Adaptive-Neuro-Fuzzy-Based Sensorless Control of a Smart-Material Actuator

Ali Sadighi, *Student Member, IEEE*, and Won-jong Kim, *Senior Member, IEEE*

***Abstract*—In this paper, adaptive-neuro-fuzzy-based sensorless control of a smart-material actuator is presented. The smart material that we used to develop a novel type of linear actuator is Terfenol-D. The peristaltic motion in the actuator is generated by inducing a traveling magnetic field inside the Terfenol-D element. The sensorless control of the actuator is based on an observation illustrating a direct relationship between the active element's position and the coils' inductances. To detect the inductance change, the coil's current response to a pulse voltage input is monitored. Then, a fundamental relationship between the coils' current-response pulsewidths and the active element's position is developed using a combination of a Sugeno fuzzy model and neural networks. Eventually, the closed-loop sensorless control of the magnetostrictive actuator was successfully performed. The neuro-fuzzy-based sensorless control demonstrated the position-estimation capability with a ±0.5-mm maximum error. The sensorless control scheme combined with the unique features of this actuator is promising in the applications, where conventional actuation and sensing methods are proved inapplicable due to technical or reliability issues.**

***Index Terms*—Adaptive-neuro-fuzzy inference system (ANFIS), fuzzy logic, magnetostrictive actuator, sensorless control.**

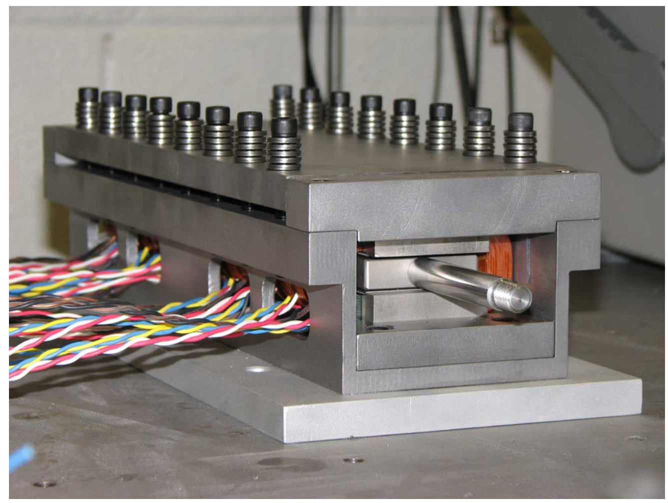

Fig. 1. Linear magnetostrictive actuator.

I. Introduction

SENSORLESS control replaces conventional sensors with position or speed estimation of motors and actuators by electrical means [1]. It finds crucial applications, where operation in harsh environments at high temperature and pressure poses a serious challenge in the reliable use of conventional sensors [2]. Most of sensorless techniques are based on a fundamental relationship between the motor's position and its magnetic characteristics. The changes in magnetic characteristics could be tracked by monitoring variables, such as current from motor's phases [3]. Besides, the phase inductance in an unenergized phase could be measured and used for position estimation [4]. In these methods, generally a probing signal has to be injected to the unenergized phases for inductance calculation. Then, the relationship between the motor's position and the phase inductance is used to estimate the position.

We developed a novel linear magnetostrictive actuator using a rectangular slab of Terfenol-D as the active element [5], as shown in Fig. 1. Terfenol-D is an alloy of formula $Tb_{0.3}Dy_{0.7}Fe_{1.92}$, which was developed by the Naval Ordnance Laboratory and has the highest magnetostriction of any alloy, up to 2000 ppm [6], [7]. Most of the commercially available magnetostrictive actuators are only capable of delivering high forces within small ranges [8], [9]. Kiesewetter conceived of the idea of generating the peristaltic motion with a Terfenol-D rod in a tight-fitting tube [10]. Later, various prototypes of inchworm motors were developed [11], [12]. Our linear magnetostrictive actuator has demonstrated the speed of 9 mm/min with the load capacity of 410 N and 45-mm travel range, and the maximum power consumption by this actuator is 95 W [5]. We also introduced the sensorless control of this actuator based on a linear approximation of the fundamental relationship between the coils' current-response pulsewidths and active element's position [13]. A position-estimation accuracy of ±1 mm was achieved using the proposed method.

The aim of this paper is to develop a neuro-fuzzy-based sensorless method for closed-loop control of a general class of magnetostrictive actuators. Based on an observation that illustrates a direct relationship between the actuator's position and the coils' inductances, a fundamental relationship was developed between the actuator's position and the coils' current-response pulsewidths. Fuzzy control and neural networks (NNs) are among most popular intelligent control techniques [14]–[16]. Fuzzy systems have the capability to approximate any continuous function [17]. Besides, fuzzy systems are known for their robustness in the sense that they are less susceptible to change in system parameters or noise [18]. Hence, we use an

Manuscript received September 10, 2009; revised December 11, 2009; accepted February 22, 2010. Date of publication March 29, 2010; date of current version January 19, 2011. Recommended by Technical Editor P. X. Liu.

The authors are with the Department of Mechanical Engineering, Texas A&M University, College Station, TX 77843-3123 USA (e-mail: a_sadighi@tamu.edu; wjkim@tamu.edu).

Color versions of one or more of the figures in this paper are available online at http://ieeexplore.ieee.org.

Digital Object Identifier 10.1109/TMECH.2010.2045004

adaptive-neuro-fuzzy inference system (ANFIS) [19] to implement this fundamental relationship.

ANFIS is a class of adaptive networks that functions as a fuzzy-inference system [20]. Since its advent, ANFIS has been extensively used in a wide variety of applications, such as modeling, signal processing, and control [19], [20]. ANFIS was employed to estimate the rotor position of a switched reluctance motor in [21]. The phase inductance of a switched reluctance motor was estimated using ANFIS in [22]. However, it is for the first time in this paper that ANFIS is employed to implement the sensorless closed-loop control of a linear magnetostrictive actuator.

In the Section II, we present the working principle and electromagnetic design of the linear magnetostrictive actuator. Section III describes the sensorless position-estimation technique. Eventually, the ANFIS-based sensorless closed-loop control of the linear magnetostrictive actuator and its experimental results are presented and discussed in Section IV. Section V describes a key application and shows the relevance and effectiveness of the proposed method.

II. Linear Magnetostrictive Actuator

The working principle of the linear magnetostrictive actuator is based on the peristaltic motion of the active element. This peristaltic motion could be induced by generating a traveling magnetic field inside the active element [5]. The active element in our design is in a rectangular shape surrounded by a force-transmission assembly. The active element is sandwiched between two thin sheets of Inconel-718, which are resistant to corrosion. The squeezing force is generated using 16 sets of Belleville spring washers and screws and transmitted to the active element through a squeezing plate. This squeezing force is transformed to the friction force between the active element and the Inconel pieces, which contributes to the reaction force required to move the active element against a load or to hold it in place. As a result, this actuator self-brakes when the power is cut off, which is one of the advantageous features of this linear magnetostrictive actuator. The stators are made of solid nickel–iron alloy 49 that has very high relative permeability of 100 000 as well as good mechanical properties ($S_{yt} = 154$ MPa), which makes it withstand normal and shear stresses due to the squeezing pressure and the external load.

The magnetic field is generated inside the active element by means of 24 prefabricated coils, where each coil consists of 273 turns of AWG#24 wire. To make the magnetic field travel, three switching boards were constructed. Each of these boards contains eight power MOSFETs and eight MOSFET drivers. The switching frequency of these boards is controlled by the digital I/Os of a DSP board (Model DS1104 by dSPACE). The objective of power electronics here is to direct the required current to three adjacent coils, and then, move it to either side depending on the actuator's motion direction. The coil arrangement and the local three-phase excitation sequence are shown in Fig. 2. Since only 3 out of 24 coils are energized at each time, the power consumption of this linear actuator is very low. The overall mass of the actuator is 14.6 kg, and its overall dimension is 86 × 72 × 320 mm. The Terfenol-D slab dimension in this actuator is 31.5 × 12.7 × 200 mm. The stator slot width is 7.9 mm, and the stator tooth thickness is 3 mm [5]. The maximum power consumption by the linear magnetostrictive actuator is 95 W, and it demonstrated that the force-generating capability of 410 N and the maximum speed is 9 mm/min [5].

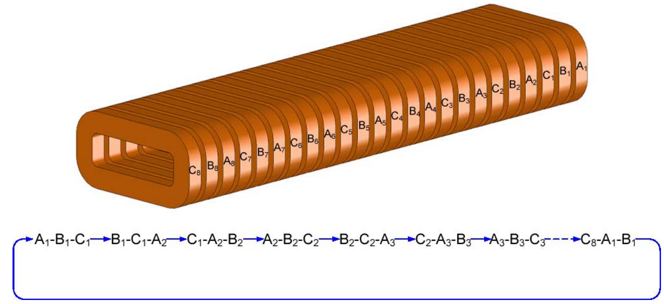

Fig. 2. Coil arrangement and local three-phase excitation sequence in the linear magnetostrictive actuator.

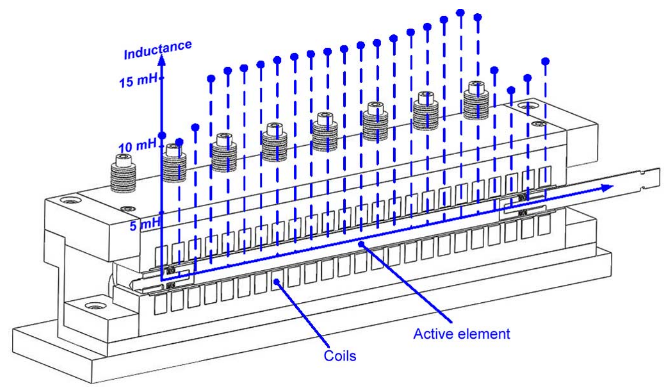

Fig. 3. Coils' inductance-measurement results with the active element placed in a predefined position illustrate the fundamental relationship between the actuator position and its magnetic characteristics.

III. Sensorless Position Estimation

A. *Fundamental Relationship*

Most sensorless methods are based on the development of a fundamental relationship between the motor position and its magnetic characteristics. In search for such a relationship in the linear magnetostrictive actuator, the active element was put in a predefined position, and the coils' inductances were measured using an *RLC* meter. The cross section of the linear magnetostrictive actuator with the active element put in a predefined position and the coils' inductances measurements are shown in Fig. 3. It is observed that the inductance of the coils, which the active element is completely through, is above 15 mH. In comparison, the inductances of other coils are around 10 mH. It is apparent that the increase in coils' inductances is due to the relative permeability of Terfenol-D of 3–10. This implies that the linear magnetostrictive actuator position can be estimated if we can detect the change in coils' inductances.

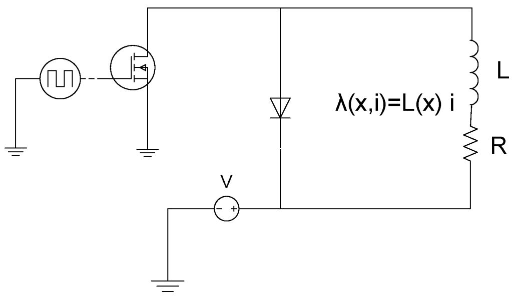

Fig. 4. Equivalent circuit of one coil.

The equivalent circuit for a single coil is shown in Fig. 4. If we apply the KVL for this circuit

$$\frac{di}{dt} \approx \frac{V - Ri}{L(x)}. \tag{1}$$

Here, we consider the system electrically linear. Besides, due to low speed of the linear magnetostrictive actuator (0.15 mm/s), the speed voltage term is neglected [23]. Since the generalized inductance of a coil is a function of position, the rate of change of the coil current is also a function of position. The responses of the two coils with different inductance values to a square-wave voltage input are shown in Fig. 5. As it is seen, by increasing the coil's inductance from 10 to 16 mH, the current-response pulsewidth rises. Thus, the current-response pulsewidth can be considered as a representation of magnetic characteristics of the linear magnetostrictive actuator. Hence, the fundamental relationship will consist of a relationship between the coils' current pulsewidth and the actuator position.

To find this fundamental relationship, we changed the active element's position from 15 to 44 mm and the current pulsewidths of the coils #3–#5 were recorded in 1-mm increments. Our choice of these three coils is due to the fact that, as the actuator moves, only these coils at either of the two ends will experience the change in inductance. The actuator movement does not affect the inductance of innermost coils because the active element is always inside these coils. To measure the coil current, we used Hall-effect-based transducers (model LA 03-PB from LEM). After reading the current from the analog-to-digital (A/D) channel of DS1104 board, the pulsewidth is calculated by measuring the area under a unity-width square wave with the length equal to the current pulsewidth. Then, the calculated pulsewidth is registered to a data storage cell as soon as the current drops to zero, which is detected by a change-detection block.

The results are depicted in Fig. 6. For each coil, there is a nonlinear curve consisting of three regions. The first is the low-magnitude area with the pulsewidth around 0.020 s. This region corresponds to the time when the active element is not inside the coil yet. Then, there is an increasing region that starts from the time the active element begins entering the coil until it is completely through the coil. Finally, each curve saturates at the pulsewidth around 0.032 s, which corresponds to the time when the active element is completely through the coil.

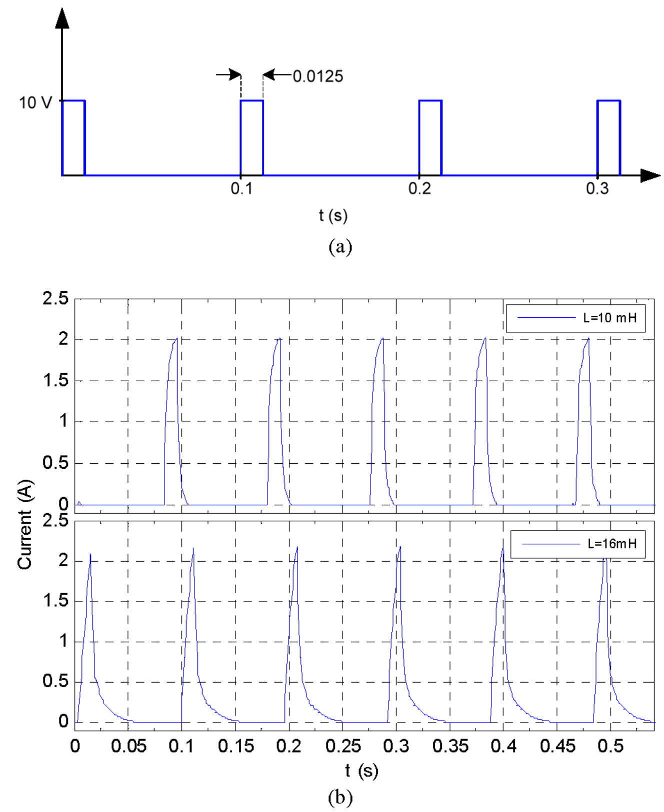

Fig. 5. (a) Voltage waveform. (b) Actual current in actuator coils with inductances of 10 and 16 mH.

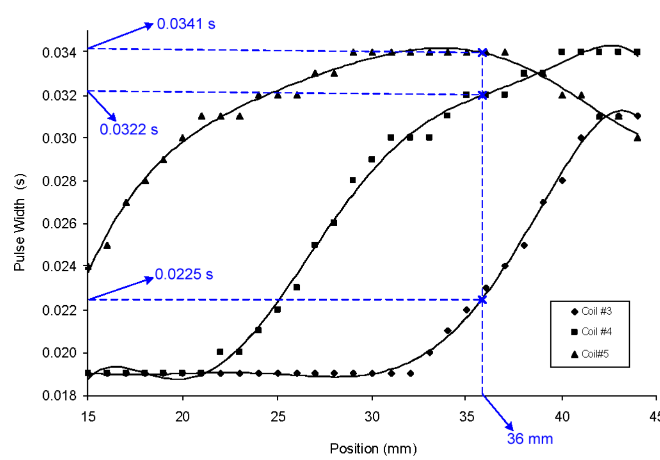

Fig. 6. Recorded current-response pulsewidths for three coils when the active element's position changes from 15 to 44 mm.

Hence, to establish the fundamental relationship, a nonlinear mapping Ψ from the current pulsewidths of three coils to the position should be created such as

$$\Psi(t_3, t_4, t_5) = x \tag{2}$$

where t_3, t_4, and t_5 are the current pulsewidths of coils #3–#5, respectively, and x is the position. As seen in Fig. 6, Ψ(0.0225, 0.0322, 0.0341) = 36 mm.

Since fuzzy systems have the capability to approximate any continuous function [17], this allows the aforementioned

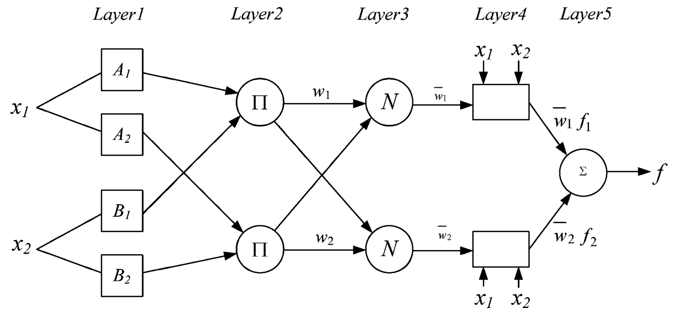

Fig. 7. Architecture of ANFIS for a fuzzy model with two inputs and one output [19].

nonlinear mapping to be modeled using a fuzzy model. Besides, fuzzy models are known for their robustness in the sense that they are less susceptible to changes in system parameters or noise [18]. If available, a mathematical model or a lookup table could also be used to create this mapping. However, the computation-intensive methods have the disadvantage of being slow, and the lookup tables need a large memory size to achieve high accuracy, and interpolations would also be necessary [24].

B. ANFIS Architecture

ANFIS [19] is a class of adaptive networks that functions as a fuzzy-inference system [20]. An ANFIS architecture for a simple Sugeno fuzzy model with two inputs x_1 and x_2 and one output *f* is shown in Fig. 7. For this Sugeno fuzzy model, two fuzzy IF–THEN rules are as follows.

Rule 1: If x_1 is A_1 and x_2 is B_1, then $f_1 = \alpha_1 x_1 + \beta_1 x_2 + \gamma_1$.

Rule 2: If x_1 is A_2 and x_2 is B_2, then $f_2 = \alpha_2 x_1 + \beta_2 x_2 + \gamma_2$.

Fuzzification of the inputs to the fuzzy model is performed in the first layer, and the outputs would be the degree of membership of each of the inputs with respect to a fuzzy set. The outputs of the adaptive nodes in this layer could be described by

$$\begin{aligned} O_{1,i} &= \mu_{A_i}(x_1), \qquad \text{for } i = 1,\, 2 \\ O_{1,i} &= \mu_{B_{i-2}}(x_2), \qquad \text{for } i = 3,\, 4 \end{aligned} \tag{3}$$

where x_1 and x_2 are the inputs to node *i*, and A_i and B_{i-2} are the fuzzy sets described by linguistic labels. The membership functions for A_i or B_{i-2} can be any appropriate parameterized ones, such as the generalized bell (or Gaussian) membership function. In this paper, the following Gaussian membership function is used:

$$\mu_{A_i}(x) = e^{-(x-c_i)^2 / 2\sigma_i^2} \tag{4}$$

where *x* is the input to the fuzzy system, and c_i and σ_i are the parameters of the membership function and referred to as premise parameters.

The second layer determines the firing strength of each rule. Each node in this layer acts as a fuzzy AND operator. If the algebraic product is used for the AND operator, the node output in the second layer will be as follows:

$$O_{2,i} = w_i = \mu_{A_i}(x_1)\mu_{B_i}(x_2), \qquad i = 1, 2. \tag{5}$$

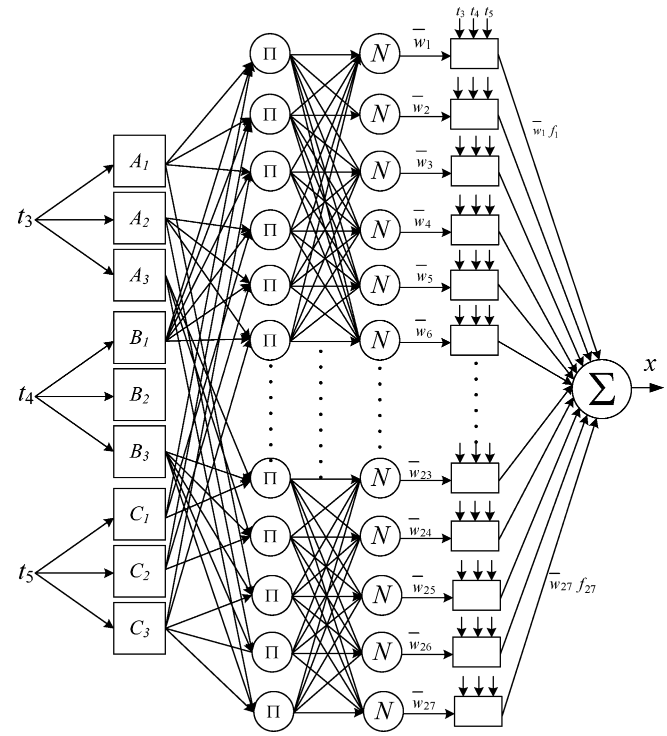

Fig. 8. Proposed ANFIS architecture for position estimation.

Normalization of firing strengths calculated in layer 3 is done in the fourth layer, and the output of each node in this layer could be described by

$$O_{3,i} = \overline{w_i} = \frac{w_i}{w_1 + w_2}, \qquad i = 1, 2. \tag{6}$$

The output of the nodes in the fourth layer is a linear combination of the inputs multiplied by the normalized firing strength

$$O_{4,i} = \overline{w_i} f_i = \overline{w_i}(\alpha_i x_1 + \beta_i x_2 + \gamma_i) \tag{7}$$

where $\{\alpha_i, \beta_i, \gamma_i\}$ are called the consequent parameters.

Finally, the outputs of the fourth layer are added in the fifth layer to generate the output of the fuzzy system.

Identification of the premise and consequent parameters is carried out using a hybrid learning algorithm. It consists of two steps, where first the consequent parameters are identified by the least-squares method in the forward pass while keeping the premise parameters fixed. Then, in the backward pass, the layer-two parameters are modified using gradient descent while the consequent parameters are held fixed.

C. Application of ANFIS for Sensorless Position Estimation

In this section, the ANFIS is employed to model the fundamental relationship between the current pulsewidths and the actuator position. The first step in training the ANFIS is to collect the data. For this purpose, we used 30 sets of data obtained earlier, as shown in Fig. 6. The ANFIS architecture is illustrated in Fig. 8. There are three inputs to the ANFIS, t_3, t_4, and t_5, which are the current pulsewidths of coils #3–#5. The input space of each variable was divided into three regions represented by three membership functions. Hence, the number of rules in

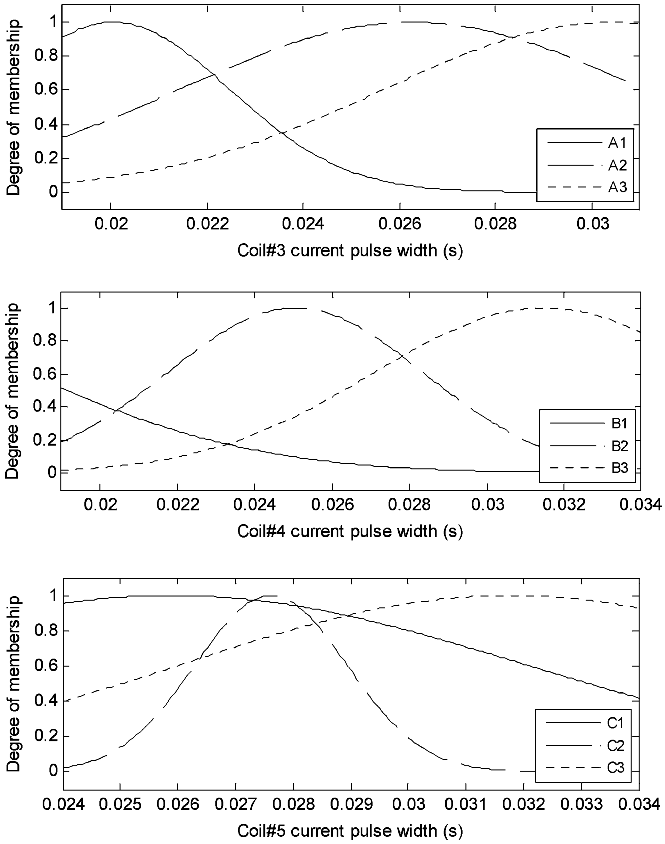

Fig. 9. Membership functions for three inputs to the ANFIS.

the fuzzy system will be 27. The Gaussian membership function is used for input variables, which is specified by two variables, as described by (4). Hence, the total number of parameters in the ANFIS that should be identified are 126, of which 18 (9×2) are the premise parameters and 108 (27×4) are the consequent parameters. The ANFIS training was performed using a hybrid optimization method, a combination of least-squares and back-propagation gradient-descent method. The optimization process continues until the training error is less than the specified error tolerance or when the maximum number of epochs is reached. Here, the error tolerance was set to zero to make sure that minimum error will be reached and the number of epochs was 100. Membership functions for each input are depicted in Fig. 9.

We also increased the number of membership functions, which barely improved the performance of the system. We also tried other types of membership functions, such as triangular and trapezoidal, but a Gaussian membership function resulted in the least amount of error.

To verify the effectiveness of the ANFIS model to estimate the position, the actuator position was changed and the measurement from a laser distance sensor was compared with the ANFIS-based actuator position. The sensorless position measurement versus the laser-distance sensor output and the error are depicted in Fig. 10. As it is seen by employing this methodology, we are able to estimate the position of the linear magnetostrictive actuator with a ± 0.5-mm maximum error.

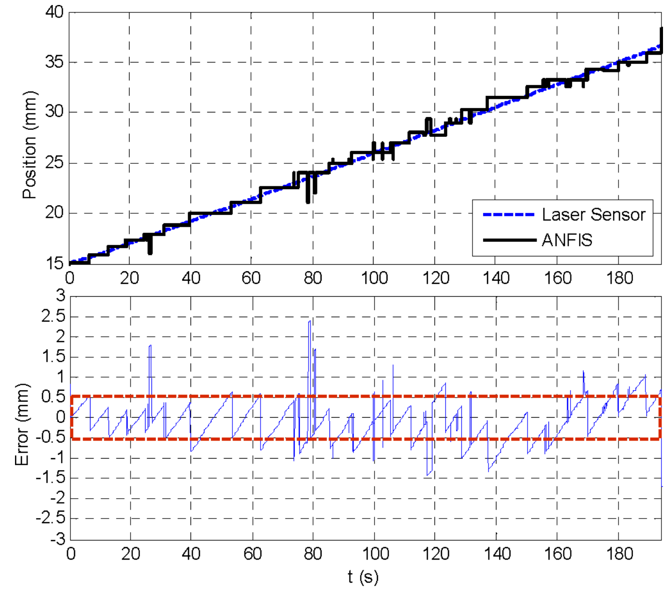

Fig. 10. Neuro-fuzzy-based sensorless position-estimation error.

This error is due to the fact that a minimum change in the active element's position should be made before a change in the current-response pulsewidth could be detected. The spikes in the ANFIS-estimated position are due to the errors in current sensing, but do not affect the closed-loop performance of the linear magnetostrictive actuator, as can be seen in Section IV.

We compared ANFIS with a feedforward NN (FFNN) and a linear method to estimate the position based on the linear approximation of fundamental relationship [13]. The developed FFNN consists of two layers with 20 neurons in the first layer and one in the output layer, and a tan–sigmoid transfer function was used for the neuron function. We used the Levenberg–Marquardt optimization method to train the network. In the linear method [13], the fundamental relationship between the current-response pulsewidths and the position was estimated linearly, and an algorithm was used to calculate the position based on these linear relationships [13]. Fig. 11 illustrates the comparison among these three methods, and Table I summarizes the rms error associated with each of three methods. It is seen that by employing a NNs (such as ANFIS or FFNN), the error is reduced by around 50%. It is due to taking into account the nonlinearities that had been neglected in the linear method [13]. On the other hand, ANFIS demonstrates less error than FFNN. Besides, since ANFIS is a combination of NNs and fuzzy Sugeno system, it has the merit of being less susceptible to changes in system parameters or noise [18].

It is seen that sensorless position estimation was built based on the coil current-response pulsewidth measurements, as shown in Fig. 6. Hence, the repeatability of these measurements plays an important role in the effectiveness of the position-estimation algorithm. To show the repeatability, three sets of measurement were performed, and the results are shown in Fig. 12. It is seen that the pulsewidth measurements are quite repeatable, and we may rely on them in estimating the position.

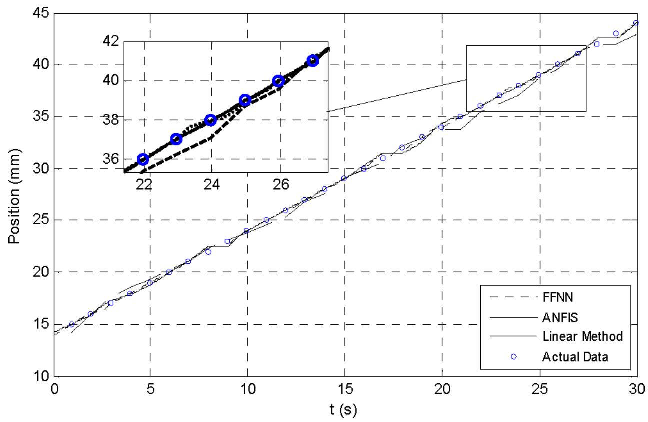

Fig. 11. Comparison among three different methods to model the fundamental relationship.

TABLE I
COMPARISON AMONG VARIOUS SENSORLESS METHODS

	ANFIS	Feed-Forward Neural Network	Linear Method
RMS Error	0.81%	0.91%	1.78%

IV. SENSORLESS CLOSED-LOOP CONTROL

Now, the ANFIS-based position-estimation algorithm can be used to implement the closed-loop control of the linear magnetostrictive actuator. A photograph of the test setup is shown in Fig. 13. The schematic diagram of control and instrumentation is shown in Fig. 14.

The coil currents are measured using Hall-effect-based current transducers, and the output voltages are sent to the A/D converters of the DSP board. Then, the current-response pulsewidths t_3, t_4, and t_5 are calculated and sent to the trained ANFIS model. The estimated position is then fed back to a relay controller with a dead zone defined as follows:

$$u = \Phi(e) = \begin{cases} +1, & e > k_0 \\ 0, & -k_0 < e < k_0 \\ -1, & e < -k_0 \end{cases} \tag{8}$$

where $\pm k_0$ defines the dead zone of the relay element. Since the precision of the position estimation is ± 0.5 mm, a dead-zone threshold value of 0.5 mm should be picked to avoid the self-oscillation [25].

Fig. 15 depicts a 5-mm closed-loop step response of the linear magnetostrictive actuator with the ANFIS-based position estimator. It is seen that the steady-state error is 0.1 mm, which is within ± 0.5 mm, as expected. This relay-based controller is also robust to the spikes present in the estimated position. This lies in the fact that the spikes are of random nature and do not always appear in the same position where actuator is operating.

Hence, although in some instances, the error signal changes due to spikes, this does not affect the control signal output from the relay controller, which is always maximum and makes the actuator move in the desired direction at the maximum speed until it reaches the vicinity of reference input, as specified by the dead-zone threshold. Fig. 16 shows the capability of the

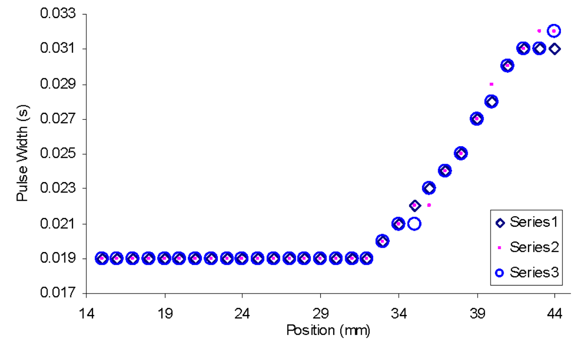

(a)

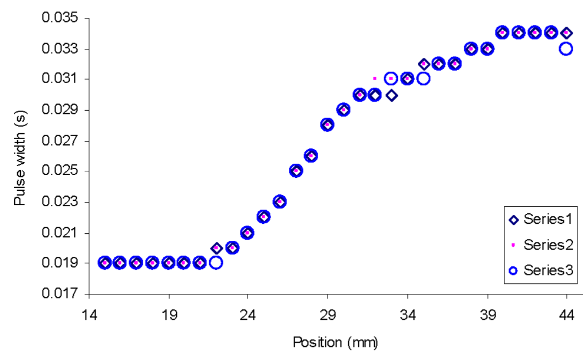

(b)

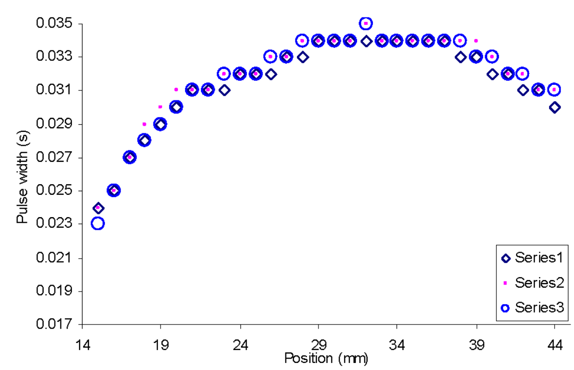

(c)

Fig. 12. Experiment for the repeatability of current-response pulsewidth measurements in (a) coil #3, (b) coil #4, and (c) coil #5.

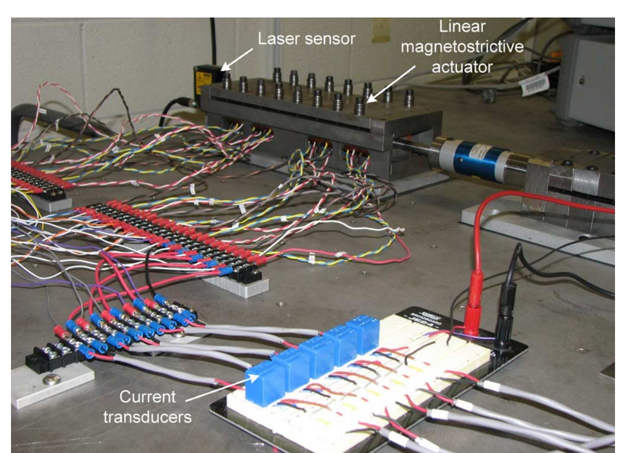

Fig. 13. Photograph of the test setup.

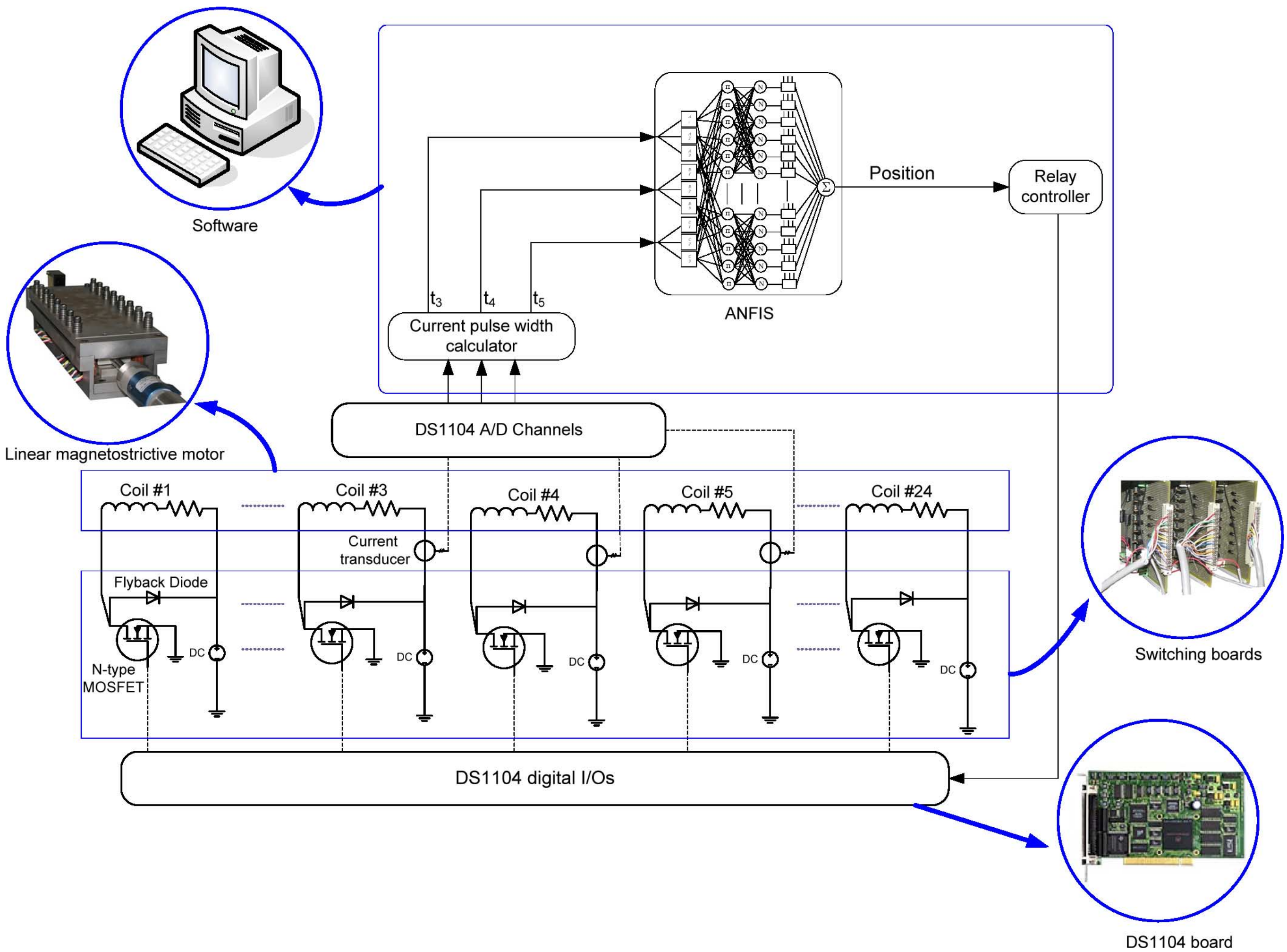

Fig. 14. Schematic control and instrumentation diagram.

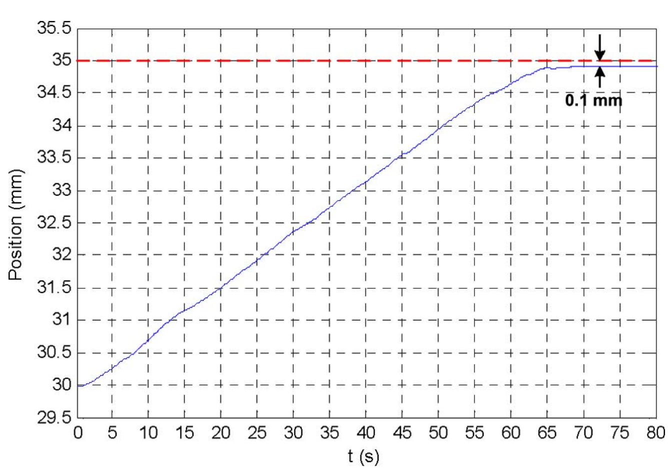

Fig. 15. Five millimeters step response of the linear magnetostrictive actuator with ANFIS-based sensorless control.

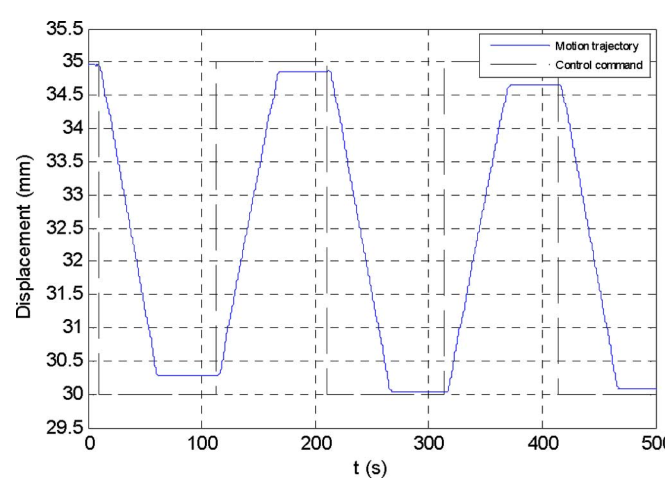

Fig. 16. Closed-loop response of the actuator to a square-wave control command.

sensorless control system in tracking a square-wave reference input. The actuator's response to a sinusoidal reference input with an amplitude of 5 mm and frequency of 0.015 rad/s is illustrated in Fig. 17.

V. Application

Recently, magnetostrictive materials have been considered for the development of novel down-hole tools. An example of such an effort is actuation of a sliding-sleeve valve (SSV) by

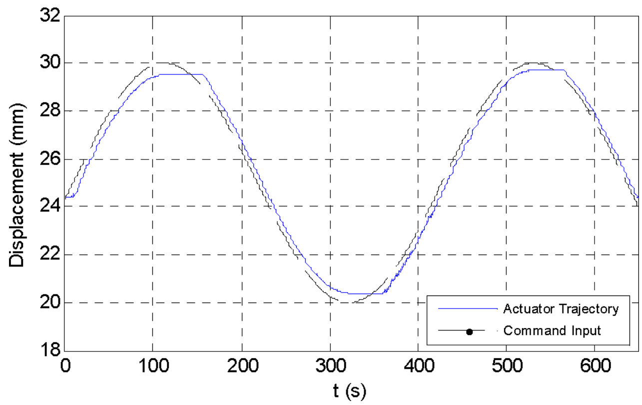

Fig. 17. Closed-loop response to a sinusoidal reference input with an amplitude of 5 mm and frequency of 0.015 rad/s.

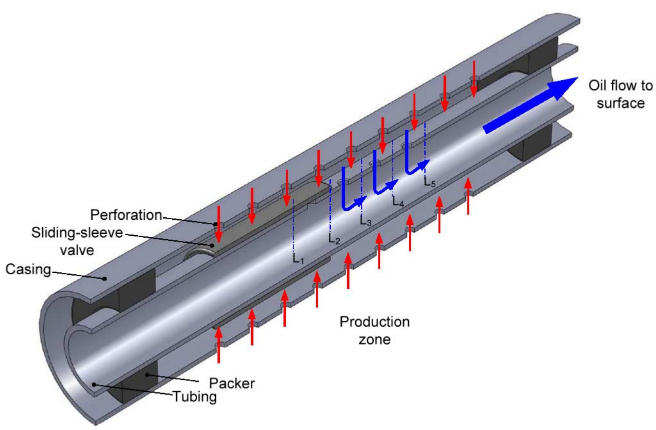

Fig. 18. Schematic drawing of SSV.

means of a linear magnetostrictive actuator [26]. An SSV is used to establish or cut off the communication between the tubing and the annulus in an oil well. A schematic cross section of an SSV is shown in Fig. 18. Oil generated from the production zone goes through perforations in casing to enter the annulus space between the casing and the tubing. This space is isolated from other production zones by two packers. Then, oil flows through ports of the SSV and enters the tubing, and then, goes up to surface for further processing. With a linear magnetostrictive actuator, the sleeve could be shifted to cover or uncover the ports machined in the body of the SSV. Using the linear magnetostrictive actuator with sensorless control has two main benefits for this application. First, the power consumption of the actuator is low, and it self-brakes when the power is cut off, which suits the power supply limitations in down-hole applications [5]. Second, the sensorless position monitoring and control eliminates the need for conventional sensors in harsh down-hole environment. It decreases the complexity and increases the reliability of the actuation system. In contrast to precision positioning applications where nanometer-level accuracy is required, the achieved ± 0.5-mm positioning accuracy exceeds the requirements for an SSV.

VI. Conclusion

We successfully implemented novel ANFIS-based sensorless control for the linear magnetostrictive actuator. First, the relationship between the inductance change in actuator coils and the rotor position was observed. Based on this observation and using different sets of experiments, a fundamental relationship between the coils' current-response pulsewidths and the actuator position was established.

Then, an ANFIS was employed to model the fundamental relationship. The proposed method illustrated a position-estimation capability of ± 0.5 mm. Eventually, the closed-loop control of the linear magnetostrictive actuator was successfully performed by feeding the ANFIS-based estimated position back to the relay controller.

The combination of the unique features of this class of actuators, i.e., self-braking and low-power consumption, combined with this newly developed sensorless control scheme is a promising alternative in applications, where conventional methods of actuation and sensing are proved inapplicable due to technical or reliability issues. An example of such an application is actuation of down-hole tools, such as SSVs. Since these types of tools require high force and low power without high-precision positioning accuracy, the proposed sensorless control method can meet their requirements well.

References

[1] A. S. Putra, S. Huang, K. K. Tan, S. K. Panda, and T. H. Lee, "Self-sensing actuation with adaptive control in applications with switching trajectory," *IEEE/ASME Trans. Mechatronics*, vol. 13, no. 1, pp. 104–111, Feb. 2008.

[2] D. Perrin, *Well Completion and Servicing*. Paris, France: Editions Technip, 1999.

[3] T. J. E. Miller, *Electronic Control of Switched Reluctance Machines*, Oxford, U.K.: Reed Educational and Professional, 2001.

[4] P. P. Acarnley, R. J. Hill, and C. W. Hooper, "Detection of rotor position in stepping and switched motors by monitoring of current waveforms," *IEEE Trans. Ind. Electron.*, vol. IE-32, no. 3, pp. 215–222, Aug. 1985.

[5] W.-J. Kim and A. Sadighi, "A novel low-power linear magnetostrictive actuator with local three-phase excitation," *IEEE/ASME Trans. Mechatronics*, vol. 15, no. 2, pp. 299–307, Apr. 2010.

[6] F. Claeyssen, N. Lhermet, and G. Grosso, "Giant magnetostrictive alloy actuators," *J. Appl. Electromagn. Mater.*, vol. 5, pp. 67–73, 1994.

[7] F. Claeyssen, N. Lhermet, R. L. Letty, and P. Bouchilloux, "Acuators, transducers and motors based on giant magnetostrictive materials," *J. Alloys Compounds*, vol. 258, pp. 61–73, Aug. 1997.

[8] J. Goldie, M. J. Gerver, J. Oleksy, G. P. Carman, and T. A. Duenas, "Composite Terfenol-D sonar transducers," in *Proc. SPIE Conf. Smart Mater. Technol.*, CA, Mar. 1999, vol. 3675, pp. 223–234.

[9] L. Kvarnsjo, "Underwater acoustic transducers based on Terfnenol-D," *J. Alloys Compounds*, vol. 258, pp. 123–125, Aug. 1997.

[10] L. Kiesewetter, "The application of Terfenol in linear motors," in *Proc. 2nd Int. Conf. Giant Magnetostrictive Alloys*, 1988, ch. 7, pp. 1–15.

[11] J. H. Goldie, M. J. Gerver, J. Kiley, and J. R. Swenbeck, "Observation and theory of Terfenol-D inchworm motors," in *Proc. SPIE Conf. Smart Struct. Integr. Syst.*, CA, Mar. 1998, vol. 3329, pp. 780–785.

[12] W.-J. Kim, J. H. Goldie, M. J. Gerver, J. E. Kiley, and J. R. Swenbeck, "Extended-range linear magnetostrictive motor with double-sided three-phase stators," *IEEE Trans. Ind. Appl.*, vol. 38, no. 3, pp. 651–659, May/Jun. 2002.

[13] A. Sadighi and W.-J. Kim, "Sensorless control of a novel linear magnetostrictive motor," in *Proc. IEEE Energy Convers. Congr. Expo. Conf.*, Sep. 2009, pp. 1726–1731.

[14] J. Huang, T. Fukuda, and T. Matsuno, "Model-based intelligent fault detection and diagnosis for mating electric connectors in robotic wiring harness assembly systems," *IEEE/ASME Trans. Mechatronics*, vol. 13, no. 1, pp. 86–94, Feb. 2008.

[15] L. Yao and P.-Z. Huang, "Learning of hybrid fuzzy controller for the optical data storage device," *IEEE/ASME Trans. Mechatronics*, vol. 13, no. 1, pp. 3–13, Feb. 2008.
[16] R.-E. Precup, S. Preitl, I. J. Rudas, M. L. Tomescu, and J. K. Tar, "Design and experiments for a class of fuzzy controlled servo systems," *IEEE/ASME Trans. Mechatronics*, vol. 13, no. 1, pp. 22–35, Feb. 2008.
[17] L. X. Wang, "Fuzzy systems are universal approximators," in *Proc. IEEE Int. Conf. Fuzzy Syst.*, San Diego, CA, Mar. 1992, pp. 1163–1169.
[18] E. H. Mamdani, "Twenty years of fuzzy control: Experience gained and lessons learnt," in *Proc. 2nd IEEE Int. Conf. Fuzzy Syst.*, 1993, vol. 1, pp. 339–344.
[19] J. S. R. Jang, "ANFIS: Adaptive-network-based fuzzy inference system," *IEEE Trans. Syst., Man, Cybern.*, vol. 23, no. 3, pp. 665–685, May 1993.
[20] J. S. R. Jang, C. T. Sun, and E. Mizutani, *Neuro-Fuzzy and Soft Computing*. Englewood Cliffs, NJ: Prentice-Hall, 1997.
[21] A. D. Cheok and Z. Wang, "Fuzzy logic rotor position estimation based switched reluctance motor DSP drive with accuracy enhancement," *IEEE Trans. Power Electron.*, vol. 20, no. 4, pp. 908–921, Jul. 2005.
[22] F. Daldaban, N. Ustkoyuncu, and K. Guney, "Phase inductance estimation for switched reluctance motor using adaptive neuro-fuzzy inference system," *J. Energy Convers. Manage.*, vol. 47, pp. 485–493, Mar. 2006.
[23] H. H. Woodson and J. R. Melcher, *Electromechanical Dynamics*. New York: Wiley, 1968.
[24] B. K. Bose, "Expert system, fuzzy logic, and neural network applications in power electyronics and motion control," *Proc. IEEE*, vol. 82, no. 8, pp. 1303–1323, Aug. 1994.
[25] W.-J. Kim and A. Sadighi, "Design and relay-based control of a novel linear magnetostrictive motor," in *Proc. Amer. Control Conf.*, Jun. 2009, pp. 3482–3487.
[26] A. P. Dorel, "Linear actuator using magnetostrictive power element," U.S. Patent 7 675 253 B2, Mar. 9, 2010.

Ali Sadighi (S'08) was born in Yazd, Iran, in 1978. He received the B.S. degree from Sharif University of Technology, Tehran, Iran, in 2000, and the M.S. degree from K.N. Toosi University of Technology, Tehran, in 2003, both in mechanical engineering. He was the recipient of the Certificate in Business from Mays Business School, Texas A&M University. He is currently working toward the Ph.D. degree in mechanical engineering at Texas A&M University, College Station.

From 2003 to 2006, he was a Design Engineer with MAPNA, Tehran. His current research interests include analysis, design, and real-time control of electromechanical systems.

Mr. Sadighi is a Student Member of the American Society of Mechanical Engineers and the Honor Society of Phi Kappa Phi.

Won-jong Kim (S'89–M'97–SM'03) received the B.S. (*summa cum laude*) and M.S. degrees in control and instrumentation engineering from Seoul National University, Seoul, Korea, in 1989 and 1991, respectively, and the Ph.D. degree in electrical engineering and computer science from Massachusetts Institute of Technology (MIT), Cambridge, in 1997.

He was with SatCon Technology Corporation, Cambridge, MA, for three years. Since 2000, he has been with the Department of Mechanical Engineering, Texas A&M University (TAMU), College Station, where he is currently an Associate Professor and the holder of the Dietz Career Development Professorship II. He is the Associate Editor of the *ASME Journal of Dynamic Systems, Measurement, and Control* and the *International Journal of Control, Automation, and Systems*. His research interests include analysis, design, and real-time control of mechatronic systems, networked control systems, and nanoscale engineering and technology. He holds three U.S. patents on precision positioning systems.

Prof. Kim is a Fellow of the American Society of Mechanical Engineers (ASME) and a member of Pi Tau Sigma. He was appointed as a Select Young Faculty Fellow by TAMU College of Engineering and the Texas Engineering Experiment Station twice in 2003 and 2005. He is a Technical Editor of the IEEE/ASME TRANSACTIONS ON MECHATRONICS. He was the recipient of the Korean Institute of Electrical Engineers' Student Paper Contest grand prize in 1988, Samsung Electronics' Humantech Thesis gold prize for his MIT dissertation in 1997, the National Aeronautics and Space Administration Space Act Award in 2002, the 2005 Professional Engineering Publishing Award for the best paper published in 2004 in the *Journal of Engineering Manufacture*, and the British Petroleum (BP) Teaching Excellence Award from TAMU College of Engineering in 2006. He was also a Semifinalist in the National Institute of Standards and Technology's Advanced Technology Program competition in 2000.